Pramana – J. Phys. (2020) 94:12
https://doi.org/10.1007/s12043-019-1867-3

Numerical and microcontroller simulations, and electronic circuit realisation of Minorsky's equation

NGOUABO ULRICH GAËL[1,2], NOUBISSIE SAMUEL[2,3,*], FOTSIN HILAIRE BERTRAND[1] and WOAFO PAUL[3]

[1]Unité de Recherche de Matière de Condensée d'Electronique et de Traitements de Signal (UR-AMCETS), Faculté des Science, Université de Dschang, B.P. 67, Dschang, Cameroun
[2]Unité de Recherche d'Ingénierie des Systèmes Industriels et Environnement (UR-ISIE), IUT-FV de Bandjoun, Université de Dschang, P.B. 134, Bandjoun, Cameroun
[3]Laboratory of Modelling and Simulation in Engineering, Biomimetics and Prototypes and TWAS Research Unit, Faculty of Science, University of Yaoundé I, P.O. Box 812, Yaounde, Cameroun
*Corresponding author. E-mail: snoubis@yahoo.fr; samuel.noubissie@univ-dschang.org

MS received 18 March 2019; revised 13 July 2019; accepted 22 August 2019

Abstract. This work deals with the mathematical analysis, numerical and microcontroller simulations and electronic circuit realisation of the dynamics of Minorsky's equation. We consider the model including the nonlinear derivative feedback with delay. The study of stability is done by linearising the equation. An alternation between the zones of stability and instability as a function of the values of the delay is found. The bifurcation diagrams allowed us to validate the analytical predictions. These bifurcation diagrams show Hopf bifurcations and complex dynamics of the system. The analog and microcontroller simulations together with the experimental analysis were carried out in order to validate the theoretical analysis.

Keywords. Minorsky's equation; nonlinear derivative feedback; time delay; complex dynamics; P-spice and microcontroller simulations; electronic circuit realisation.

PACS Nos 05.45.−a; 05.45.Pq

1. Introduction

The dynamical systems with delay have received great attention over the past decade, due to their applications in various fields such as physics, mathematics, biology, economics, engineering, etc. [1–6]. The presence of delay in a system increases the degree of freedom and nonlinearity of the system which may give rise to various complex dynamics such as chaos, hyperchaos, etc.

During the last decades, we observe that the scientists are showing particular interest to propose control systems with delay for electromechanical structures such as ships and rotating machines [1]. Thus, many researchers proposed the proportional and/or derivative control systems with delay by carrying out analytical studies [7–9]. Moreover, they showed that the proposed models can show different complex behaviours such as periodicity, quasiperiodicity and chaos; all these depending on the gain of the controller. Many other researchers worked in the same line, notably Wang *et al* [10] and Siewe *et al* [11] who analytically and numerically studied the global dynamics of the Duffing's oscillator with a delayed proportional feedback. Using basins of attraction, they defined different areas of stability and instability. On the other hand, Johnson and Moon [12] and Buscarino *et al* [13] focussed their studies on the experimental aspect of electromechanical systems with delayed feedback. They proposed miniaturised models to observe the aforementioned complex behaviours. Buscarino *et al* [14], Biswas and Banerjee [15], and many other researchers [16–20] showed their interest in the delayed dynamical systems, by proposing an analog circuit. They showed that the obtained electronic calculators can present stability, limit cycles and even chaotic phenomena. However, Ablay [21] revealed that the delayed analog circuit can fully play its role only when the input signals have just one frequency. Chiu *et al* [22] and Murillo-Escobar *et al* [23] showed that it is possible to analyse the dynamical systems by using microcontrollers. But, they did not take into account the presence of delay which is important in real applications. Motivated by the aforementioned

Published online: 18 December 2019

Table 1. Delay intervals for regions of stability and instability around the equilibrium point as a function of b.

τ	$b = 0.11$	$b = 0.2$	$b = 0.5$
τ_1	]0; 2.65[	]0; 1.92[	]0; 1.39[
τ_2	]2.65; 2.77[	]1.92; 2.28[	]1.39; 2.26[
τ_3	]2.77; 8.79[	]2.28; 7.68[	]2.26; 632[
τ_4	]8.79; 9.20[	]7.68; 9.13[	]6.32; 10.27[
τ_5	]9.20; 14.93[	]9.13; 13.44[	]10.27; 11.25[
τ_n	–	–	–

works, in this work, we intend to compare the theoretical analysis, microcontroller simulations and experimental results based on electronic circuit corresponding to the Minorsky's equation.

The present work is organised as follows: in §2, a description of the model and stability analysis of the model are given. A numerical simulation of the system is presented in §3 and the obtained results are compared with those given by the analog and experimental (§4) and microcontroller simulations (§5). The conclusion is given in §6.

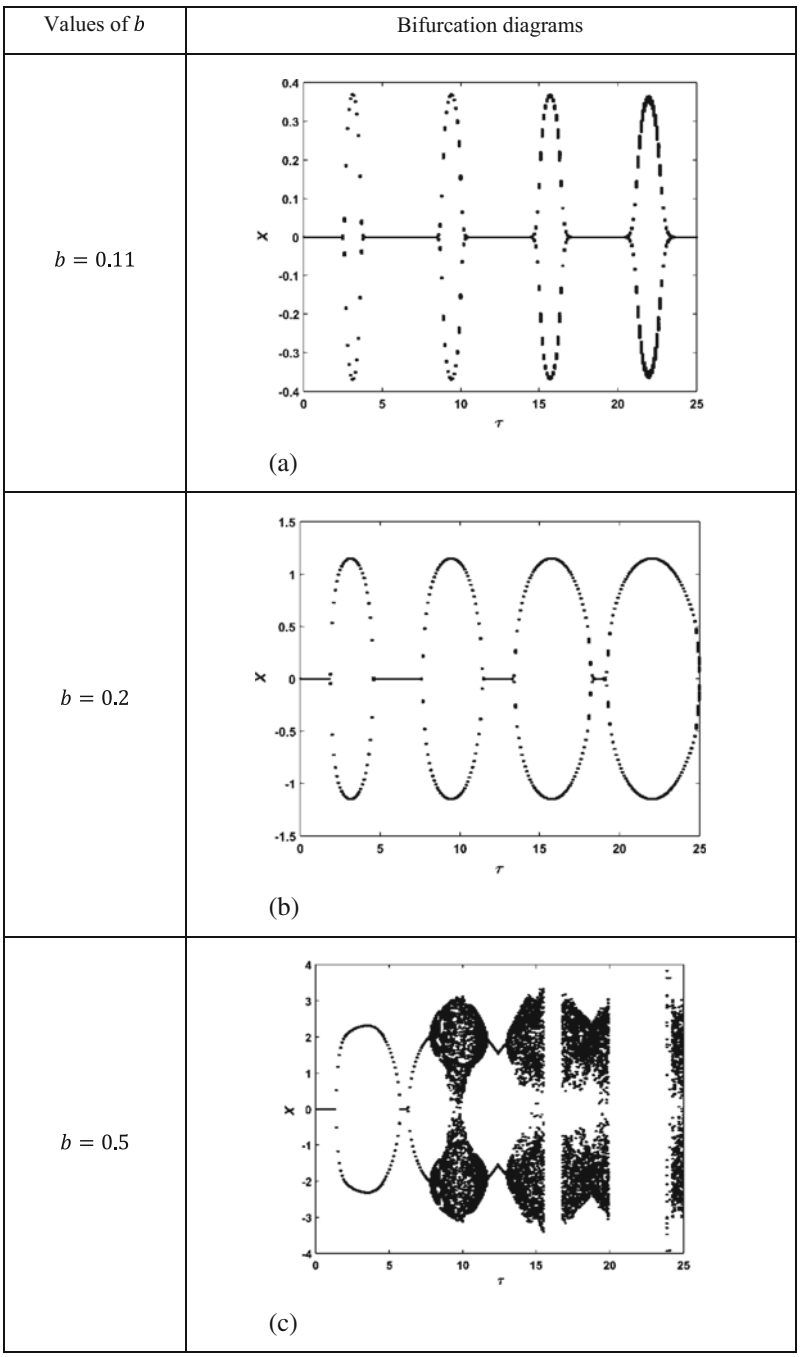

Figure 1. Bifurcation diagrams of $x(\tau)$ for different values of b.

2. Description of the model and stability analysis

2.1 *Description of the model*

The Minorsky's equation is given by the following expression [1]:

$$\ddot{y}(t) + a\dot{y}(t) + y(t) = -b\dot{y}(t-\tau) + \varepsilon\dot{y}^3(t-\tau), \quad (1)$$

where y is the swept angle, a is the damping coefficient, b and ε are positive constants which represent respectively the linear and nonlinear derivative gain of the controller. The delay τ simply expresses the action time of the controller.

Equation (1) can be rewritten as follows:

$$\begin{cases} \dot{x} = -ax - y - bx(t-\tau) + \varepsilon x^3(t-\tau), & (2a) \\ \dot{y} = x. & (2b) \end{cases}$$

Equations (2a) and (2b) represent respectively the temporal evolution of position and speed.

Despite this equation is derived from a mechanical system, its electronic equivalent can be interesting because of the complex behaviours that can be generated by varying the electronic components. This is why this work considers such an electronic circuit which is simulated using analog electronic components, but also using microcontroller simulation.

2.2 *Stability analysis*

The point $A(0, 0)$ is an equilibrium point of eq. (2). The characteristic equation of the linearised form of eq. (2) related to this equilibrium point is given as follows:

$$\lambda^2 + (a + be^{-\tau})\lambda + 1 = 0. \quad (3)$$

Substituting $\lambda = i\omega$ (ω is a real parameter) into eq. (3), one obtains the following equations:

$$\begin{cases} b\omega\sin(\omega\tau) = \omega^2 - 1, & (4a) \\ b\omega\sin(\omega\tau) = -a\omega. & (4b) \end{cases}$$

These equations lead to

$$\omega^4 - (2 - a^2 + b^2)\omega^2 + 1 = 0. \quad (5)$$

Calculating the discriminant of eq. (5), two real solutions ω_+^2 and ω_-^2 of the same sign are obtained only if

$$(2 - a^2 + b^2)^2 - 4 > 0 \quad (6)$$

and are defined as follows:

$$\omega_\pm^2 = \frac{1}{2}\left(2 - a^2 + b^2 \pm \sqrt{(2 - a^2 + b^2)^2 - 4}\right). \quad (7)$$

Moreover, these solutions are positive only if

$$\left(2 - a^2 + b^2\right) > 0. \quad (8)$$

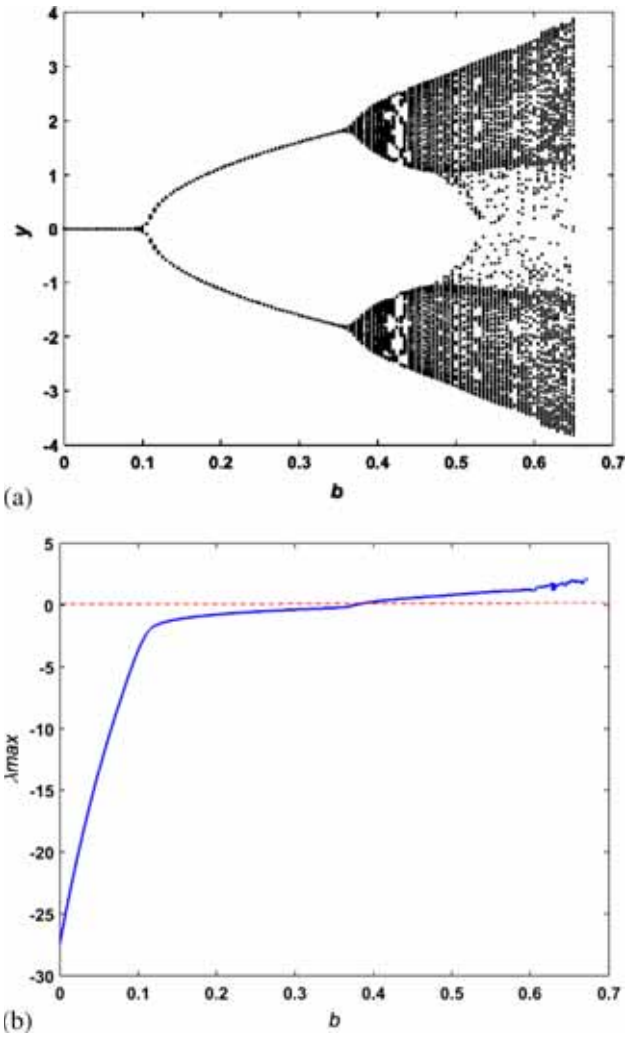

Figure 2. Bifurcation diagram (**a**) and maximum Lyapunov exponent (**b**) of y as a function of b for $\tau = 9$.

When conditions (6) and (8) are satisfied, to conclude about the stability of equilibrium point, one needs to look for different values of delay τ. Considering eq. (4b), one can find the following expression of τ_n:

$$\tau_n = \frac{1}{\omega_\pm}\left(\arccos\left(-\frac{a}{b}\right) + 2\pi n\right) \quad (9)$$

with $n \in \mathbb{N}$.

Thus, eq. (9) will give the intervals of delay, where the system will be stable and unstable following the odd and even values of n.

For instance, considering the following values of the parameters, $a = 0.1$ and $\varepsilon = 0.1$, the system is stable around the equilibrium point $A(0, 0)$ for different values of delay given in table 1.

Table 1 shows the delay intervals of stable and unstable regions for the indexes of τ odd and even. One can also observe that the increase in the derivative gain b reduces the stability intervals.

Values of b	Different time traces and phase portraits for $\tau = 9$
$b = 0.05$	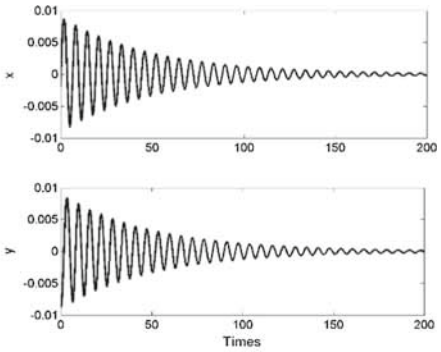 (a)
$b = 0.3$	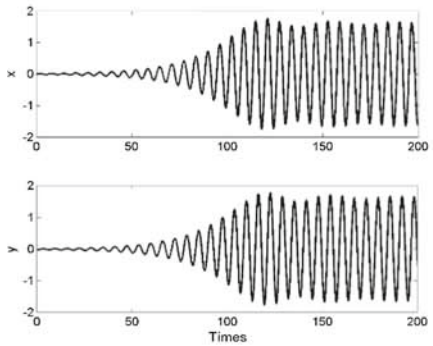 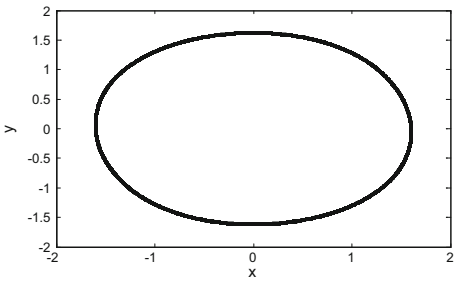 (b) (c)
$b = 0.5$	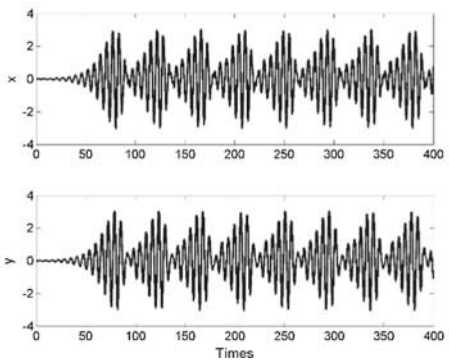 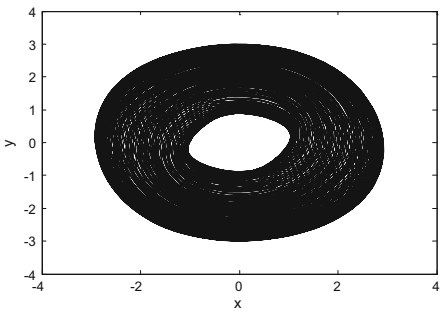 (e) (d)

Figure 3. Time series and phase portraits for different values of b.

3. Numerical simulations

To verify the results obtained analytically, we solve eq. (2) numerically with the help of the fourth-order Runge–Kutta algorithm (RK4). With the initial conditions used as $(0.1; 0.1)$, we plotted the bifurcation diagram as a function of delay to observe the effect of derivative gain and delay on the global dynamics of System (2).

Figure 1 shows that for small values of the derivative gain b (such as $b = 0.11$), the increase in delay leads to an alternation between the stability and instability regions as we observed with the analytical results.

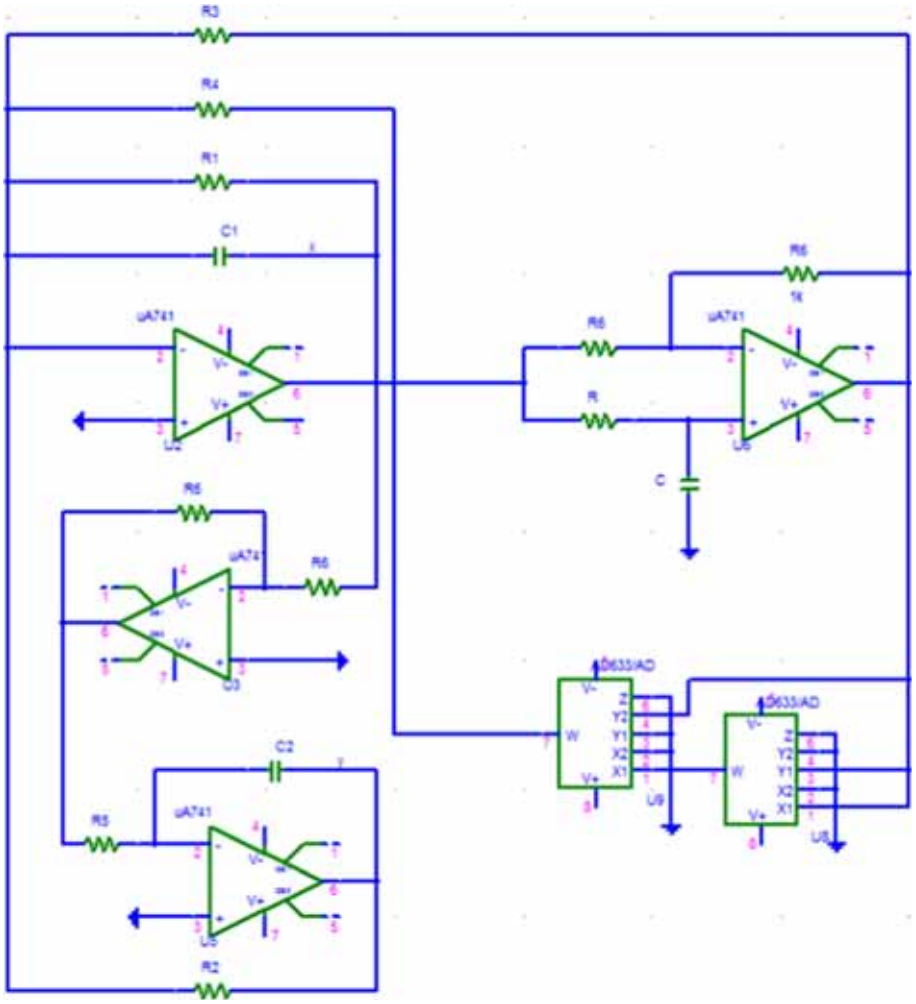

Figure 4. Analog circuit of the Minorsky's equation (2).

Due to this fact, we also observe the appearance of Hopf bifurcation points, which is referred to as the transition from the convergence of the trajectories of the system (for example from an equilibrium point to a limit cycle). Moreover, the increase in the value of the derivative gain b contributes to the reduction of the stability regions (the region where the trajectories converge to the equilibrium point) and to the increase in the instability regions (the region where we observe a limit cycle) as we observed analytically. This increase in the region of the limit cycle leads to the appearance of quasiperiodic and chaotic behaviours with the increase of delay as we observe when $b = 0.5$.

The bifurcation diagram (figure 2) shows that for certain values of gain of the controller, the system presents regions where the trajectories converge to the equilibrium point, the limit cycle and even the chaotic states. This is verified by the maximum Lyapunov exponent and the various phase portraits and time traces given in figure 3.

4. Analog simulation and experiment

4.1 *Analog simulation*

In this section, an electronic circuit of the considered model is proposed to mimic the different behaviours observed in figure 3 for the parameters $a = 0.1, \varepsilon = 0.1$ and $\tau = 9$. Figure 4 presents such an analog circuit describing the Minorsky's equation (eq. (1)). Indeed, applying the Kirchhoff laws, the circuit of figure 4 is described by the following equations:

$$\begin{cases} \dfrac{\mathrm{d}x}{\mathrm{d}t} = -\dfrac{1}{R_1 C_1 \omega_0} x - \dfrac{1}{R_2 C_1 \omega_0} y \\ \qquad\qquad -\dfrac{1}{R_3 C_1 \omega_0} x\,(t-\tau) + \dfrac{1}{R_4 C_1 \omega_0} x^3 (t-\tau), \qquad (10a) \\ \dfrac{\mathrm{d}y}{\mathrm{d}t} = \dfrac{1}{R_5 C_2 \omega_0} x. \qquad (10b) \end{cases}$$

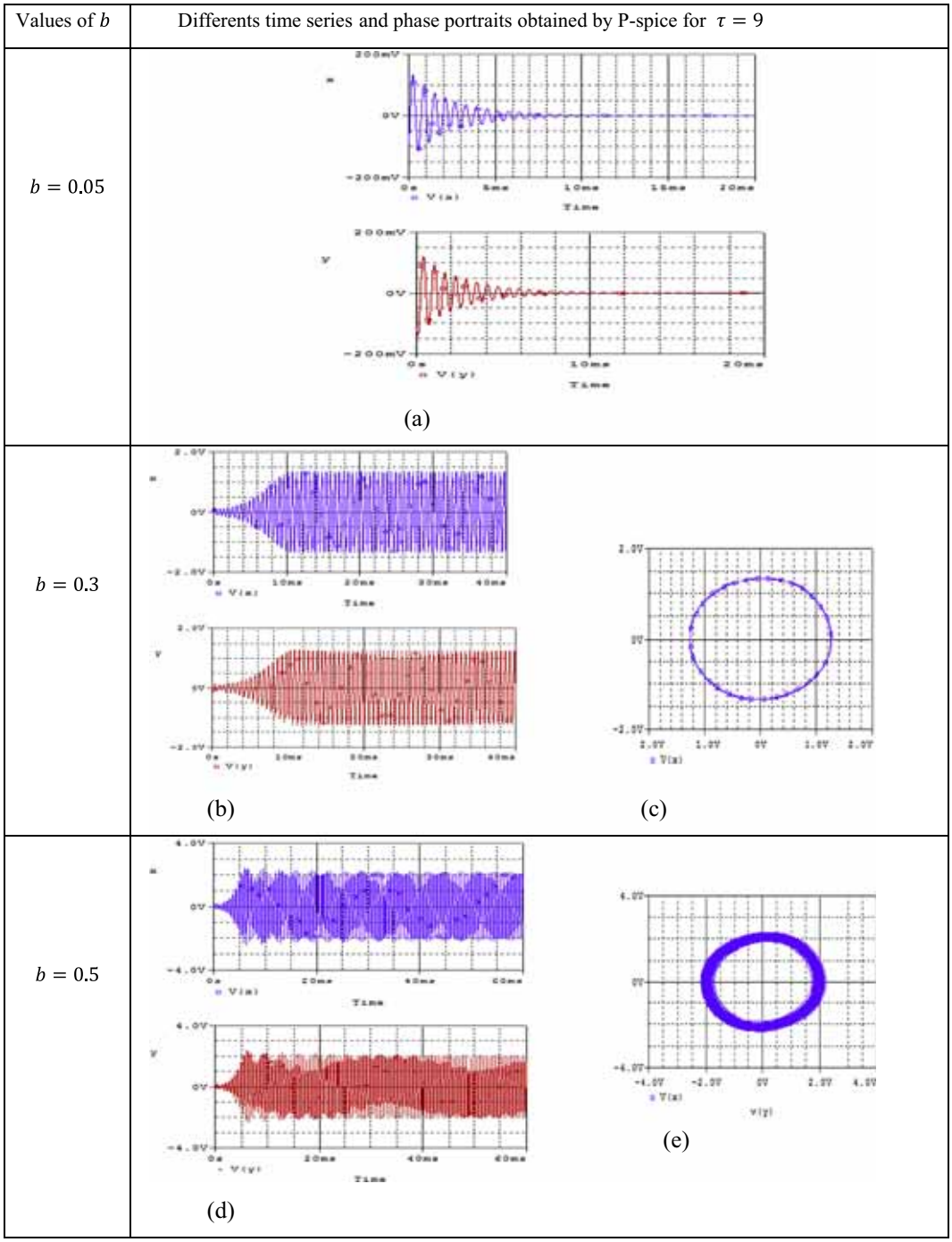

Figure 5. Time series and phase portraits of System (2) obtained by analog simulation for $\tau = 9$.

The variables of the system correspond to the output voltages of capacitors C_1 and C_2. The cubic nonlinearity is realised using two multipliers (AD633/AD) and the delayed terms are built by using the first order of a pass-all filter. The other components are chosen to correspond to eq. (2) and are given as follows:

$$R_1 = 100\,\text{k}\Omega;\ \ R_2 = 10\,\text{k}\Omega;\ \omega = 10^4;\ R_3 = 20\,\text{k}\Omega;$$
$$R_4 = 1\,\text{k}\Omega;\ \ R_5 = R_6 = 10\,\text{k}\Omega;\ C_1 = C_2 = 10\,\text{nF},$$

R_3 is a variable and $\tau = nRC$,

where n represents the number of blocks, R and C are used to obtain the desired delay.

The phase portraits and time series obtained by the P-spice simulation confirm that the proposed analog circuit reproduces the same dynamics observed using the numerical simulations. They are presented in figure 5. This confirmation is obtained for the following

Values of b	Differents time series and phase portraits obtained by P-spice for $\tau = 10$
$b = 0.5$	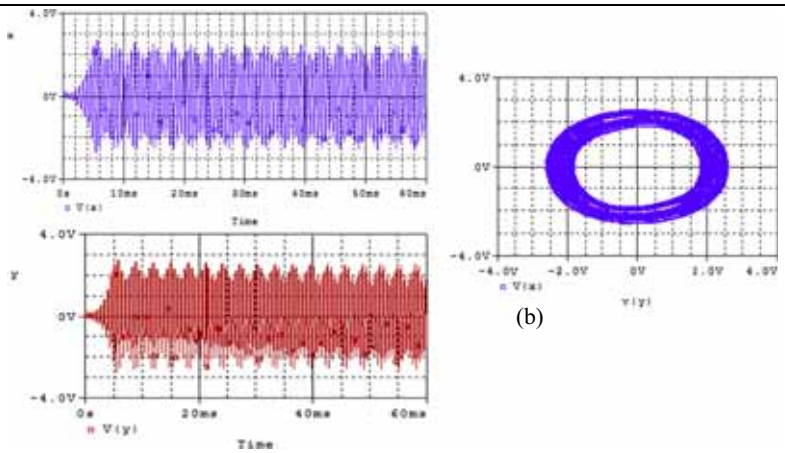 (a) (b)

Figure 6. Time series and phase portrait of System (2) obtained by analog simulation for $\tau = 10$.

Values of b	Different time series and phase portraits obtained by microcontroller simulation
$b = 0.05$	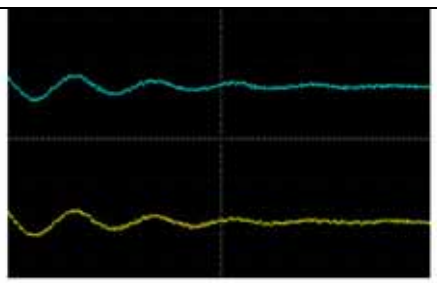 (a)
$b = 0.3$	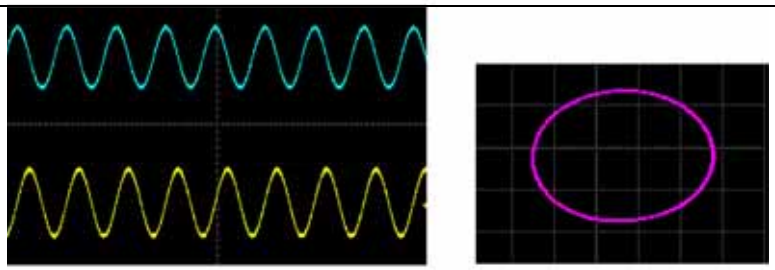 (b) (c)
$b = 0.5$	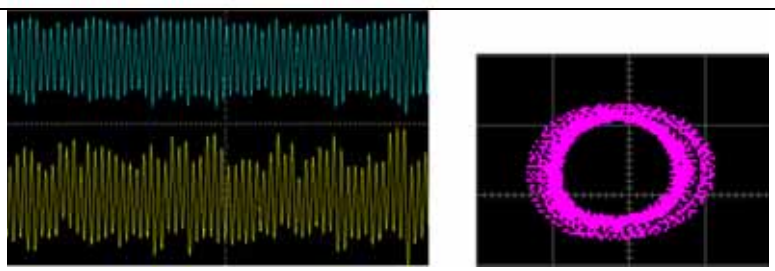 (d) (e)

Figure 7. Experimental time series and phase portraits of Minorsky's equation on the oscilloscope.

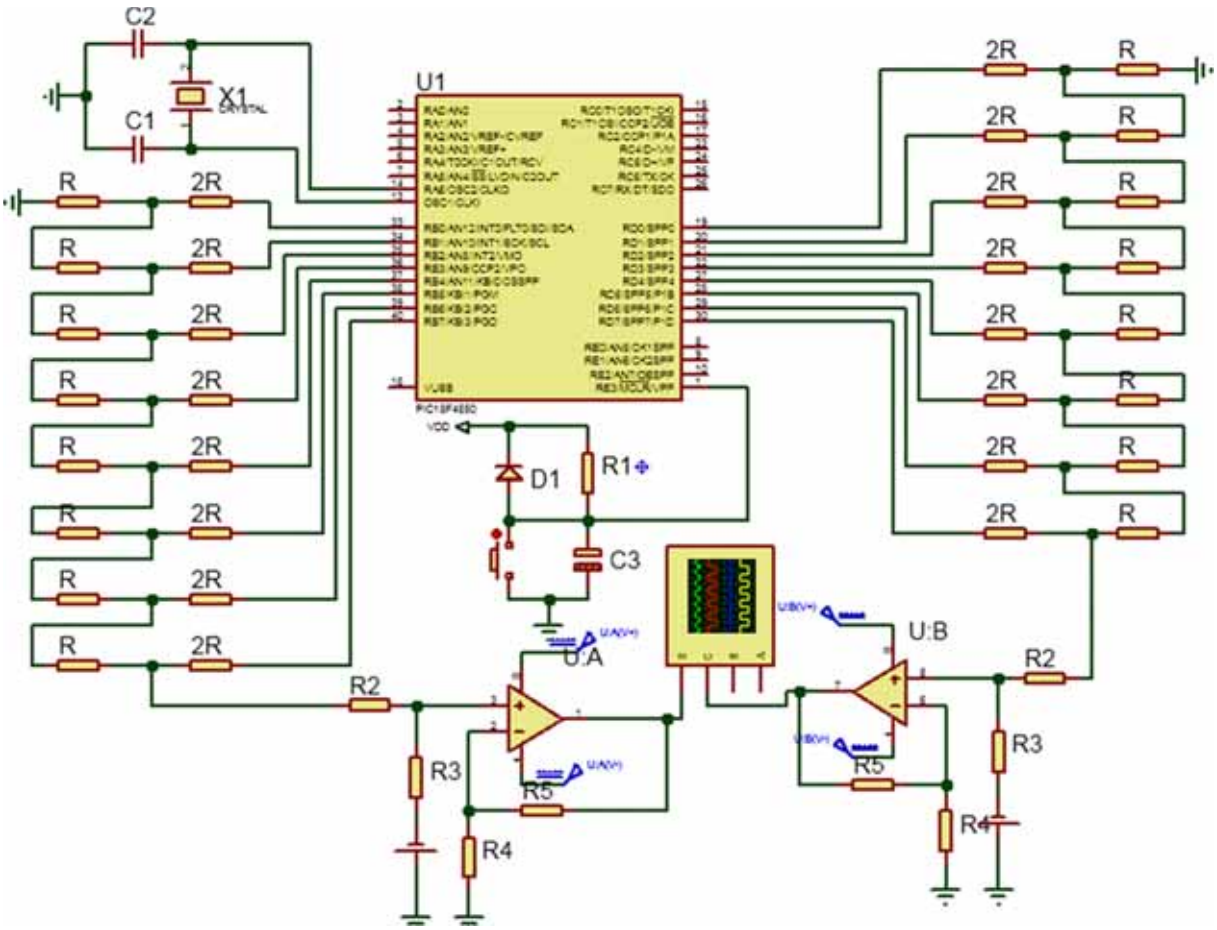

Figure 8. Microcontroller set-up for the implementation of System (2).

parameter values: $b = 0.05$, $b = 0.3$ and $\tau = 9$. However, for $b = 0.5$ and $\tau = 9$ the numerical equivalent is perceptible analogically, when $\tau = 10$ as illustrated in figure 6. This incoherence justifies the fact that the pass-all filter used here as delayed circuit plays its role effectively when the input signal has only one frequency [21]. However, the result obtained numerically at $\tau = 9$ is rather obtained analogically for $\tau = 10$ as one can observe in figure 6.

4.2 *Experiment using the analog circuit*

To validate the results obtained by numerical and P-spice simulations, it is necessary to carry out experimental studies. This experimental study is necessary because it allows us to confirm the phenomena observed during the numerical analysis and gives the possibility to use the proposed circuit in a specific domain of engineering. The results obtained are grouped in figure 7 with $\tau = 10$ and b taken as the control parameter.

The time series (figures 7a and 7b) and phase portrait (figure 7c) are obtained by considering the delay $\tau = 9$. The time trace and the phase portrait presented respectively by figures 7d and 7e are obtained for $\tau = 10$. Figure 7 shows a concordance of the results obtained by the numerical and P-spice simulations.

5. Microcontroller simulation

In this section, we aim to find the numerical and analog results by using the microcontroller simulations that will fulfil the shortcomings of analog circuits with delay. The technique is also chosen for its simplicity and ease in implementation [24–27]. The microcontroller used here is a PIC 18F4550 from Microchip® to which we have associated an R-2R resistances network acting as a digital-analog converter. This simulation is done to visualise the values of the variables x and y sent by the microcontroller through ports B and D by using an oscilloscope. The circuit consisting of capacitors $C_1 = C_2 = 33$ pF, and the quartz makes it possible to schedule the rhythm of the execution of algorithm. The two stages offset are identically made up of one

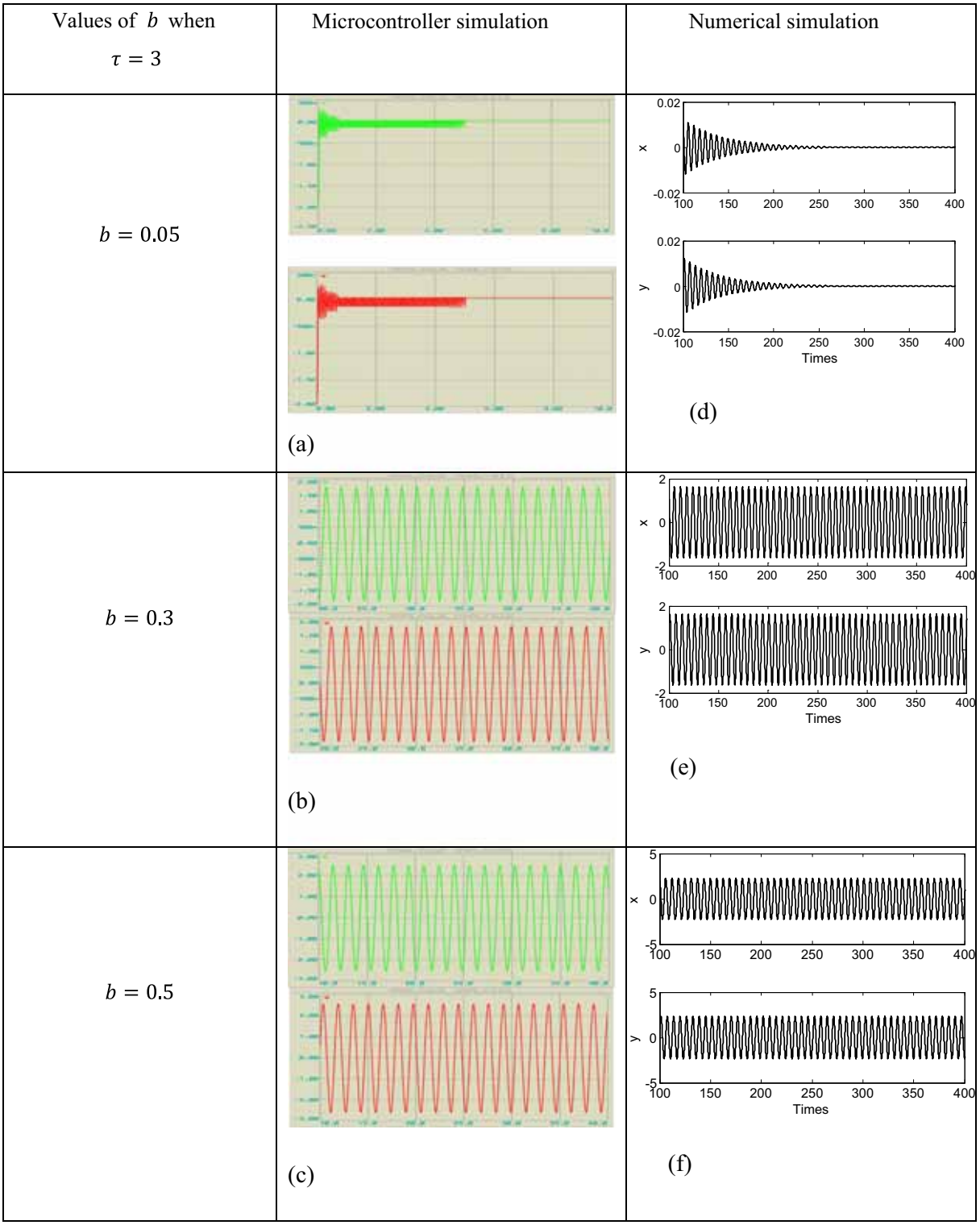

Figure 9. Comparison between the curves obtained by the numerical and microcontroller simulations for different values of b when $\tau = 3$.

TL082 operational amplifier, resistors $R_2 = 43\,\text{k}\Omega$ and $R_3 = R_4 = R_5 = 10\,\text{k}\Omega$. The reset circuit comprises the D1 1N4148 diode, the resistor $R_1 = 10\,\text{k}\Omega$, the capacitor $C_3 = 1\,\mu\text{F}$ and the push button. The diagram is illustrated in figure 8.

The Runge–Kutta algorithm (RK4) is used for the simulation through the software MikroC Pro version 6.6.3. The algorithm implemented in the microcontroller consists of two main loops. The first loop performs the Runge–Kutta algorithm for a time interval from

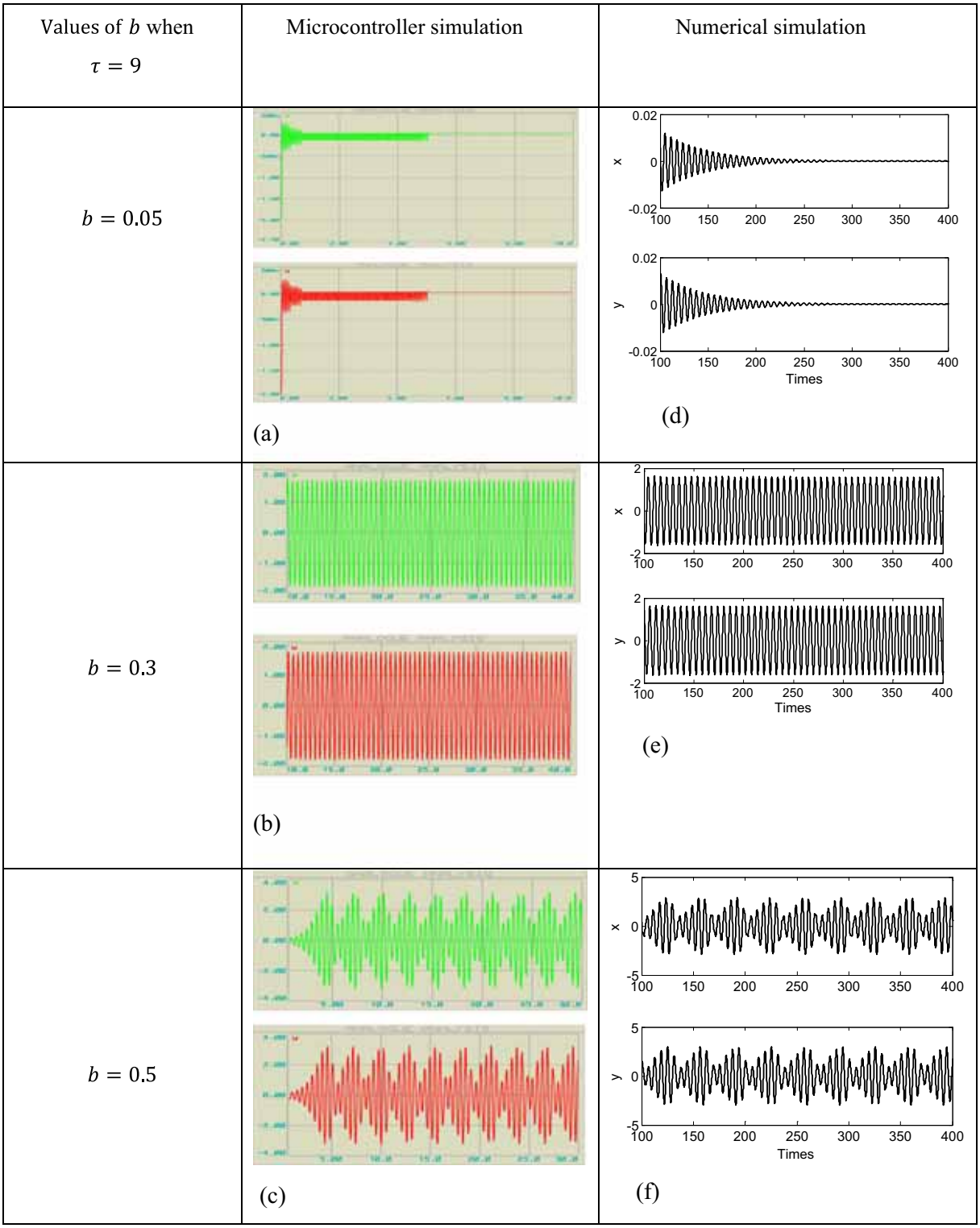

Figure 10. Comparison between the curves obtained by the numerical and microcontroller simulations for different values of b when $\tau = 9$.

0 to the value τ, the different values of the system states are recorded. In the second infinite loop, we execute the algorithm taking the previous recorded values as initial conditions. Ports B and D are configured to send x and y to the outside of the microcontroller. The different behaviours observed are represented in figures 9 and 10.

The time series obtained in figures 9 and 10 using the microcontroller simulation clearly show the good agreement with the curves obtained by numerical simulations.

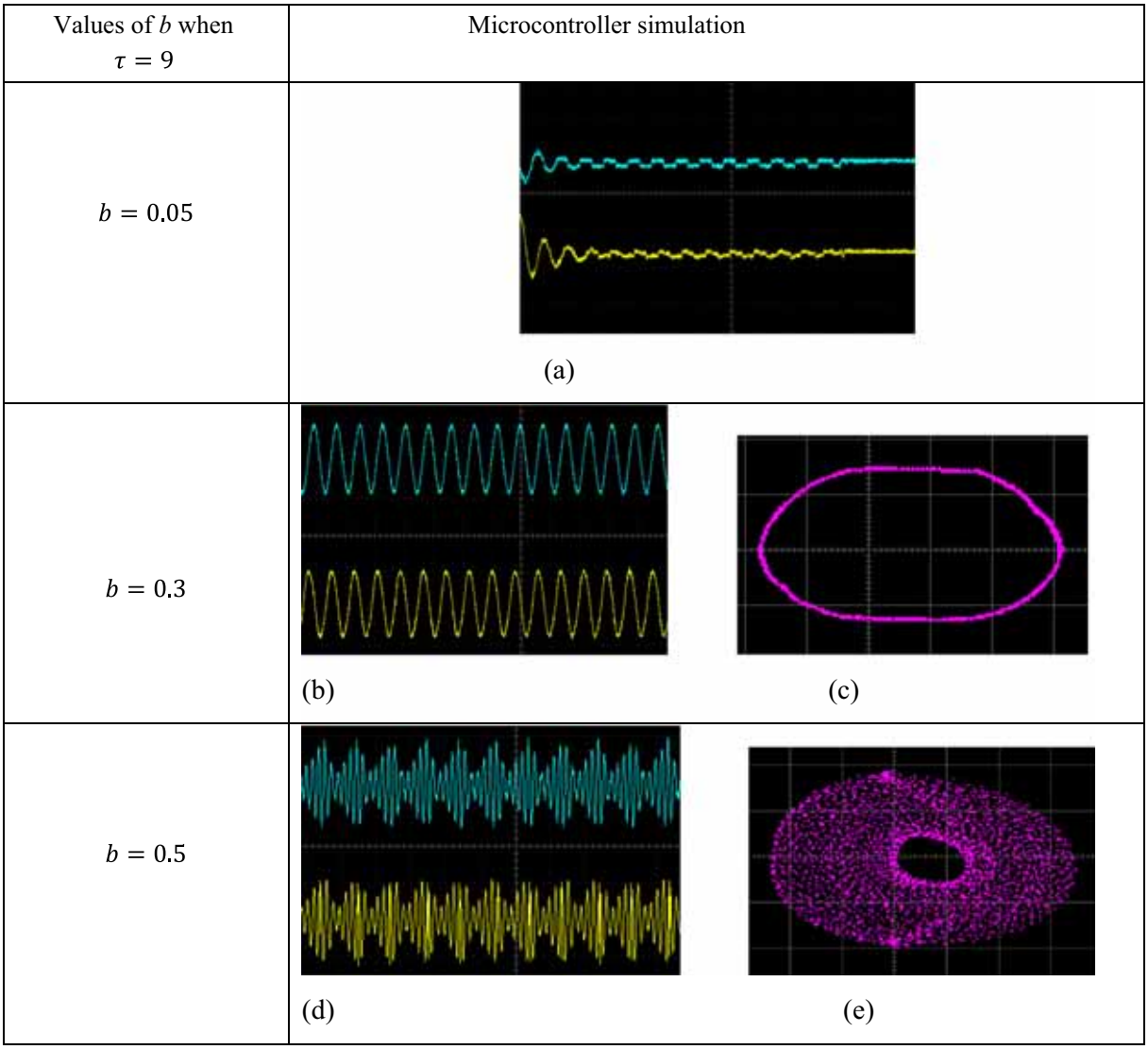

Figure 11. Time series and phase portrait of System (2) experimentally obtained by the microcontroller simulation for different values of b when $\tau = 9$.

Thus, the use of microcontroller simulation solves the problem of delayed signal with the multiple frequencies observed using the analog simulation. It is noted that when the value of the delay becomes important ($\tau = 9$ for example), simulation by the microcontroller of the considered system is no longer possible because its storage capacity is limited. To circumvent this difficulty, we have resized System (2) by setting $t' = t/3$, in order to observe the different behaviours exhibited at $\tau = 9$ in the reduced time intervals (figure 10).

In order to get the actual signals, let us now implement the diagram proposed in figure 8. The different results observed at the oscilloscope are given in figure 11.

A comparison between figures 10 and 3 shows a good agreement for different values of control parameters b when $\tau = 9$. The experimental results obtained by the electronic circuit (figure 7) and by the microcontroller (figure 11) simulations when compared to figure 3 show clearly a better approximation of those obtained by microcontroller simulation. This is because the electronic component values are not exact due to external factors. The results obtained here confirm the validity of the microcontroller embedded technology to convert the nonlinear equations of any dynamical system into electrical signals of different types.

6. Conclusion

In this work we have studied the delayed Minorsky's equation. The analytical, numerical, microcontroller simulations and electronic circuit realisation of the model were carried out. The analytical method allowed us to determine the intervals of the delay parameter where the system is stable or unstable. It has been found

that the increase in the derivative gain b reduces the zones of stability for the fixed point. The numerical simulations have confirmed the analytical predictions and also have indicated that the increase in the value of the derivative gain leads to complex phenomena in the dynamics of the system. The results obtained by microcontroller simulation and electronic circuit realisation are in good agreement with those obtained by numerical simulation.

References

[1] T Erneux, *Applied delay differential equations* (Springer, 2008)

[2] M C Mackey and L Glass, *Science* **197(4300)**, 287 (1977)

[3] O M Kwon, J H Park and S M Lee, *Nonlinear Dyn.* **63**, 239 (2011)

[4] T Banerjee, D Biswas and B C Sarkar, *Nonlinear Dyn.* **72**, 321 (2013)

[5] E M Miandoab, H N Pishkenari, A Yousefi-Koma and F Tajaddodianfar, *Int. J. Eng. Sci*. **82**, 74 (2014)

[6] H Farokhi and M H Ghayesh, *Int. J. Eng. Sci.* **91**, 12 (2015)

[7] G I Koumene Taffo, M Siewe Siewe and C Tchawoua, *Chaos Solitons Fractals* **87**, 226 (2016)

[8] P Nwagoum Tuwa and P Woafo, *J. Vib. Control* **24**, 2020 (2018)

[9] L Wang, W B Liu and H L Dai, *Int. J. Eng. Sci.* **75**, 79 (2014)

[10] H Wang, H Hu and Z Wang, *Int. J. Bifurc. Chaos* **14**, 2753 (2004)

[11] R T Siewe, A F Talla and P Woafo, *Int. J. Nonlinear Sci. Numer. Simul.* **18**, 515 (2017)

[12] M A Johnson and F C Moon, https://doi.org/10.1142/S0218127499000031 (2011)

[13] A Buscarino, C Famoso, L Fortuna and M Frasca, *Int. J. Bifurc. Chaos* **26**, 1650161 (2016)

[14] A Buscarino, L Fortuna, M Frasca and G Sciuto, *IEEE Trans. Circuits Syst. I: Regul. Pap.* **58**, 1888 (2011)

[15] D Biswas and T Banerjee, *Nonlinear Dyn.* **83**, 2331 (2016)

[16] V K Tamba, S T Kingni, G F Kuiate, H B Fotsin and P K Talla, *Pramana – J. Phys.* **91**: 12 (2018)

[17] O S Iyiola and F D Zaman, *Pramana – J. Phys.* **87**: 51 (2016)

[18] Z Wei, K Rajagopal, W Zhang, S T Kingni and A Akgül, *Pramana – J. Phys.* **90**: 50 (2018)

[19] J Banerjee, U Ghosh, S Sarkar and S Das, *Pramana – J. Phys.* **88**: 70 (2017)

[20] S T Kingni, J R M Pone, G F Kuiate and V-T Pham, *Pramana – J. Phys.* **93**: 12 (2019)

[21] G Ablay, *Nonlinear Dyn.* **81**, 1795 (2015)

[22] R Chiu, M Mora-Gonzalez and D Lopez-Mancilla, *IERI Procedia* **4**, 247 (2013)

[23] M A Murillo-Escobar, C Cruz-Hernández, F Abundiz-Pérez and R M López-Gutiérrez, *Microprocess. Microsyst.* **45**, 297 (2016)

[24] K S Ojo, A O Adelakun and A A Oluyinka, *Pramana – J. Phys.* **92**: 77 (2019)

[25] R T Siewe, U S Domguia and P Woafo, *Int. J. Nonlinear Sci. Numer. Simul.* **19**, 153 (2018)

[26] A E Giakoumis, C K Volos, I N Stouboulos, I K Kyprianidis and V-Y Pham, *International Conference on Modern Circuits and Systems Technologies (MOCAST)* (IEEE, 2017)

[27] M E Tekougoum, U G Ngouabo, S Noubissié, H B Fotsin and P Woafo, *Commun. Nonlinear Sci. Numer. Simul.* **62**, 454 (2018)